Multimode excitation of stimulated Raman scattering in spherical particles. Angular characteristics of scattered radiation

A.A. Zemlyanov, Yu.E. Geints, and E.K. Chistyakova

Institute of Atmospheric Optics,
Siberian Branch of the Russian Academy of Sciences, Tomsk
Received April 22, 1999

In this paper we consider how the multimode excitation of stimulated Raman scattering in a spherical particle influences the angular distribution of radiation intensity in the far zone. It is shown that at multimode excitation of the SRS the directional pattern becomes asymmetric in contrast to the case when a single resonance mode of the particle participates in this process. The degree of asymmetry significantly depends on the combination of modes excited in the particle. This causes either a significant increase in the intensity of the wave scattered in the backward direction or its weakening in this direction. The results are compared with those for the case of elastic scattering.

Introduction

As shown in numerous experimental and theoretical studies, a transparent micrometer-size particle can act, when exposed to an intense laser radiation, as a source of coherent radiation at Raman frequencies because of different nonlinear optical effects of light scattering in the particle's volume [stimulated Raman scattering (SRS), stimulated Brillouin scattering (SBS), stimulated fluorescence (SF), etc.]. This causes the interest in the studies of the processes of stimulated scattering of light in microparticles and opens up wide prospects for different applications of these effects to diagnostics of aerosols,[1,2] Raman microspectroscopy,[3–5] and laser technology.[6–9]

The angular distribution of radiation scattered from a micrometer-size particle has theoretically been studied in Ref. 10. It was shown that the angular pattern of scattered radiation, when "supported" by only one of its resonance modes, is symmetric in the forward and backward directions. This angular distribution follows from the corresponding symmetry of the spatial distribution of the field of the emitting mode of stimulated scattering in a particle and characterizes just the unimodal regime of stimulated scattering. Geints and Zemlyanov (Ref. 10) have also estimated the angular behavior of the intensity of scattering at multimode excitation of the stimulated scattering in a particle. It turned out that in this case the directional pattern deforms: it extends forward along the direction of pump radiation similarly to the angular distribution of the elastic scattering. However, in contrast to the latter, the angular structure of the field of stimulated scattering is characterized by a lower symmetry of the forward–to-backward intensity ratio and by a far deeper dip at the scattering angles near $\theta \approx 90°$.

This paper continues the studies discussed in Ref. 10. It considers the regularities of the angular distribution of the field of stimulated scattering from transparent particles under conditions of multimode excitation in a more detail.

The physical mechanism of excitation of stimulated scattering in a spherical particle is associated with the presence of natural electromagnetic modes with high Q-factor in it.[11] If one component of the Raman "noise" spectrum falls in resonance with a natural mode of a droplet oscillations, then amplification of this wave dominates over the absorption; thus establishing the conditions favoring the stimulated scattering. One of the peculiarities of the resonance spectrum of large particles is high density of natural modes on the frequency scale. The mean distance between modes of the same polarization (Te or TM) and of the same order M, for example, for a water droplet with the diffraction parameter $x_a = 50$ is $\Delta\nu \sim 10^{-2}$ cm^{-1}. The halfwidth of these modes c_{nl} varies within $10^{-4} \le c_{nl} \le 10^{-1}$ cm^{-1}. Consequently, the resonance curves of some natural modes can intersect (Fig. 1), and several resonance modes of a particle can participate in the amplification of a spontaneous signal to the stimulated one.

Basic equations

Let us consider the problem under study in the following formulation. Let a spherical particle with the dielectric constant ε_a is exposed to the plane electromagnetic wave incident along the positive direction of the axis z. The vector of the electric field is $\mathbf{E}_0(x, y, z; t) = \tilde{\mathbf{E}}_0(x,y)\, e^{i\omega t - ikz}$. When in the particle this wave excites the field of stimulated scattering with the electric vector $\mathbf{E}_S(\mathbf{r}', t)$ at the frequency ω_S. The problem is to find the intensity of the field of stimulated scattering at the point with the radius vector $\mathbf{r}$ outside the particle. The geometry of the problem is shown in Fig. 2.

0235-6880/99/07 575-07 $02.00

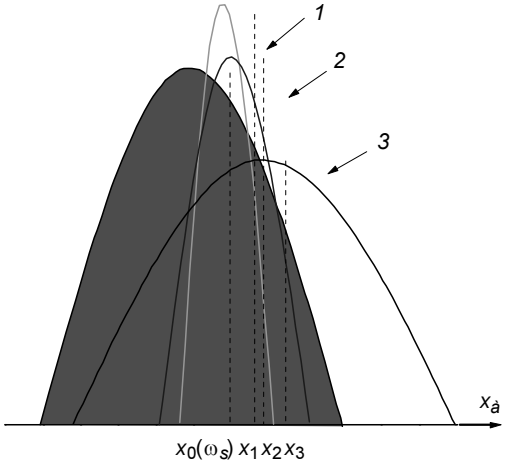

Fig. 1. Scheme of the positions of resonance contours of natural electromagnetic modes of a spherical particle at a multimode excitation of stimulated scattering: contours of the TE_{81}^{1}-mode (*1*), TE_{75}^{2}-mode (*2*), and TE_{66}^{4}-mode (*3*). The shaded contour is the basic resonance mode TE_{70}^{3}.

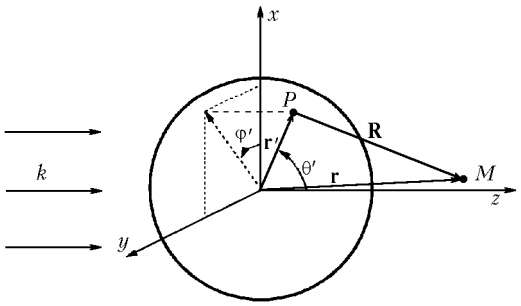

Fig. 2. Geometry of the problem on scattering of a light wave by a spherical particle.

Our considerations starts from Helmholtz equation for the vector potential of the electromagnetic field $\mathbf{A}(\mathbf{r}, t)$ at the frequency of Raman scattering[12]:

$$\Delta\mathbf{A}(\mathbf{r}, t) + k^2\,\mathbf{A}(\mathbf{r}, t) = -\,\mathbf{J}_a(\mathbf{r}, t) \qquad (1)$$

under the condition that div $\mathbf{A}(\mathbf{r}, t) = 0$, which is valid in the absence of free charges in the particle. Here $\mathbf{J}_a(\mathbf{r}, t) = \varepsilon_a \dfrac{\partial \mathbf{E}_S(\mathbf{r}, t)}{\partial t}$ is the density of polarization currents induced by the internal field of the particle; ε_a is the dielectric constant of the particle; k is the wave number. The components of the sought electromagnetic field can be expressed through the vector potential as

$$\mathbf{H}_S(\mathbf{r}, t) = \mathrm{rot}\,\mathbf{A}(\mathbf{r}, t)\ ; \quad \mathbf{E}_S(\mathbf{r}, t) = -\frac{\partial \mathbf{A}(\mathbf{r}, t)}{\partial t}\ .$$

The solution to Eq. (1) is known.[9] The electric field $\mathbf{E}_S(\mathbf{r}, t)$ at an arbitrary point in space can be found from the following equation[13]:

$$\varepsilon_a\,\mathbf{E}_S(\mathbf{r}, t) = \mathrm{rot\ rot} \int\limits_{V_a} \frac{(\varepsilon_a - 1)\,\mathbf{E}_S(\mathbf{r}', t)\,\mathrm{e}^{-ikR}}{4\pi R}\,\mathrm{d}\mathbf{r}', \quad (2)$$

where $R = |\mathbf{r} - \mathbf{r}'|$ is the distance between the point of observation and the elementary source within the particle. The integral is taken over the whole volume occupied by the sources of scattered waves (the particle volume V_a).

Taking into account that $R = \sqrt{r^2 + (r')^2 - 2r\,r'\cos\gamma} \approx$ $\approx r - r'\cos\gamma$ and interchanging the operations of integration and differentiation, we have in the far zone ($kr \gg 1$, $r \gg r'$) that

$$\mathbf{E}_S(\mathbf{r}, t) \approx \frac{k^2(\varepsilon_a - 1)}{4\pi r} \exp\{i\omega_s t - ikr\} \times$$
$$\times \int\limits_{V_a} \mathbf{E}_S(\mathbf{r}', t)\, e^{ik_a r' \cos\gamma}\,\mathrm{d}\mathbf{r}'. \qquad (3)$$

Here $k_a = \sqrt{\varepsilon_a}k$ is the wave number inside the particle; γ is the angle between the vectors $\mathbf{r}$ and $\mathbf{r}'$, $r = |\mathbf{r}|$. Note that the radial component of the electric field $E_r \ll (E_\theta, E_\varphi)$, and thus of the field far from the particle is a diverging transverse spherical wave formed by superposition of fields emitted by the polarized elements of the particle volume.

Similar integral equation can be derived for another vector component of the electromagnetic field $\mathbf{H}_S(\mathbf{r}, t)$. The main advantage of this approach to determination of the spatial structure of the field of stimulated scattering over the traditional method for solution of the differential equations for Debye potentials used in Mie theory[14] is that the integral equation (3) itself contains its boundary conditions. Therefore, any change in the shape of a scatterer does not change the structure of solution (3) but changes only the limits of integration.

In the general case integral equation (3) can be solved, for example, by the method of successive approximations.[13] However, we believe that the spatial distribution of the field of stimulated scattering in the particle corresponds to the structure of the field of one natural resonance mode of the particle, that is, the unimodal excitation of stimulated scattering takes place. Then we can write

$$\mathbf{E}_S(\mathbf{r}, t) = \frac{A_E(t, k_a a)}{k_a r}\,\psi_n(k_a r)\,\mathbf{M}_{n1}(\theta, \varphi) +$$
$$+ \text{complex conjugated}$$
$$\text{for } TE_n\text{-modes},$$
$$\mathbf{E}_S(\mathbf{r}, t) = \frac{A_M(t, k_a a)}{k_a r}\,\frac{1}{k_a}\,\nabla\,[\mathbf{M}_{n1}(\theta, \varphi)\,\psi_n(k_a r)] +$$
$$+ \text{complex conjugated}$$
$$\text{for } TM_n\text{-modes}, \qquad (4)$$

where a is the particle radius; A_E and A_M are some amplitude coefficients determining the time behavior of the process of stimulated scattering and dependent on the resonance properties of a selected mode; $\mathbf{M}_{n1}(\theta, \varphi)$ are the spherical vector–harmonics[15]; ψ_n are Ricatti–Bessel functions. The specific form of the coefficients A_E and A_M can be found from solution of the set of related equations for the main and Stokes waves in the particle.[16]

To make calculations more convenient, let us expand Eq. (4), for example for the TM_n-mode, over spherical components ($\mathbf{e}_r$, $\mathbf{e}_\theta$, $\mathbf{e}_\varphi$):

$$\mathbf{E}_S(\mathbf{r}, t) = \frac{A_M(t, k_a a)}{k_a r} \times$$

$$\times \left[\frac{n(n+1)}{k_a r} \psi_n(k_a r) \cos\varphi \sin\theta \, \pi_{n1}(\theta) \, \mathbf{e}_r + \right.$$

$$\left. + \psi_n'(k_a r) (\cos\varphi \, \tau_{n1}(\theta) \, \mathbf{e}_\theta - \sin\varphi \, \pi_{n1}(\theta) \, \mathbf{e}_\varphi)\right], \quad (5)$$

where $\pi_{n1}(\theta)$ and $\tau_{n1}(\theta)$ are the angular functions:

$$\pi_{nl}(\theta) = \frac{P_{nl}(\cos\theta)}{\sin\theta};$$

$$\tau_{nl}(\theta) = \frac{\partial}{\partial\theta}[P_{nl}(\cos\theta)],$$

$P_{nl}(\cos\theta)$ are the adjoint Legendre polynomials.

Let us also present the exponent in the integrand of Eq. (3) as a sum of spherical functions (using the theorem of summation[17]):

$$e^{ik_a r\cos\gamma} = \sum_{m=0}^{\infty} i^m (2m+1) \, j_m(k_a r) \, P_m(\cos\gamma), \quad (6)$$

where $j_m(k_a r) = \frac{1}{k_a r} \psi_m(k_a r)$ is Bessel spherical function.

Taking into account that

$$\cos\gamma = \cos\theta\cos\theta' + \sin\theta\sin\theta'\cos(\varphi - \varphi')$$

and applying the expansion formula, which is well-known from the theory of Legendre functions,[17]

$$P_m(\cos\gamma) = \{P_m(\cos\theta) \, P_m(\cos\theta') +$$

$$+ 2\sum_{l=1}^{m} \frac{(n-m)!}{(n+m)!} P_{ml}(\cos\theta') \, P_{ml}(\cos\theta') \cos[m(\varphi - \varphi')]\},$$

we transform Eq. (6) as:

$$e^{ik_a r\cos\gamma} = \sum_{m=0}^{\infty} i^m (2m+1) j_m(k_a r) \{P_m(\cos\theta) \, P_m(\cos\theta') +$$

$$+ 2\sum_{l=1}^{m} \frac{(m-l)!}{(m+l)!} P_{ml}(\cos\theta) \, P_{ml}(\cos\theta') \cos[m(\varphi - \varphi')]\}. \quad (7)$$

Upon substitution of Eqs. (5) and (7) into the integral (3), the equation for the spherical component of the electric field, for example along the unit vector $\mathbf{e}_\theta$, takes the form

$$E_\theta(\mathbf{r}, t) = \frac{k^2(\varepsilon_a - 1)}{4\pi r} \exp\{i\omega_s t - ikr\} \frac{A_M(t, k_a a)}{k_a^2} \times$$

$$\times \sum_{m=0}^{\infty} i^m (2m+1) \int_0^{2\pi} \cos\varphi' \, d\varphi' \int_0^{\pi} \tau_{j1}(\theta') \{\tau_{n0}(\theta) \pi_{n0}(\theta') +$$

$$+ 2\sum_{l=1}^{m} \frac{(n-l)!}{(n+l)!} \tau_{nl}(\theta) \pi_{nl}(\theta') \cos[m(\varphi - \varphi')]\} \sin(\theta') \, d\theta' \times$$

$$\times \int_0^a \psi_n(k_a r') \, \psi_n'(k_a r') \, dr'. \quad (8)$$

As seen, the equation derived involves the integrals of the form

$$\int_0^{2\pi} \cos\varphi' \cos[m(\varphi - \varphi')] \, d\varphi' = \begin{cases} 0 & \text{at } m \neq 1 \\ \pi\cos\varphi & \text{at } m = 1. \end{cases}$$

Then

$$E_\theta(\mathbf{r}, t) = (i)^n (2n+1) \exp\{i\omega_s t - ikr\} \times$$

$$\times \frac{A_M(t, k_a a)(\varepsilon_a - 1)}{2 k_a r} \cos\varphi \, \tau_{n1}(\theta) \, \Re_{1(nn)}, \quad (9)$$

where $\Re_{1(nj)} = \int_0^a \psi_n'(k_a r) \, \psi_j(k_a r') \, dr'$. When deriving Eq. (9), we took into account the fact that the angular functions τ_{n1} and π_{n1} are orthogonal. The equation for the component of the sought field along the axis $\mathbf{e}_\varphi$ has the following form:

$$E_\varphi(\mathbf{r}, t) = -(i)^n (2n+1) \exp\{i\omega_s t - ikr\} \times$$

$$\times \frac{A_M(t, k_a a)(\varepsilon_a - 1)}{2 k_a r} \sin\varphi \, \pi_{n1}(\theta) \, \Re_{1(nn)}. \quad (10)$$

Remind that the mode index n points at the particular natural electromagnetic mode supporting the process of formation of the stimulated scattering wave in the particle. For the TE_n resonance modes of the particle, the equations for the spherical components of the field of stimulated radiation are similar to Eq. (10) upon the replacement of the coefficients $A_M \to iA_E$; $\pi_{j1}(\theta) \leftrightarrow \tau_{j1}(\theta)$; $\Re_{1(nj)} \to \Re_{2(nj)}$, where

$$\Re_{2(nj)} = \int_0^a \psi_n(k_a r) \, \psi_j(k_a r') \, dr'.$$

The coefficients $\Re_{1(nn)}$ and $\Re_{2(nn)}$ represent the actual thickness of the emitting layer in the particle.

As follows from Eqs. (9) and (10), the angular dependence of the components of the vector $\mathbf{E}_S$ outside the particle is the same as inside it. Generally speaking, this would be expected starting from the requirement of continuity of the tangential components of the field when passing through the particle surface.

The intensity of SRS radiation from the particle for the TM_n natural modes is

$$I(\theta, \varphi, t) = I_\theta + I_\varphi =$$

$$= (2n+1)^2 \, |\Re_{1(nn)}|^2 \, \frac{c|A_M(t, k_a a)|^2 (\varepsilon_a - 1)^2}{32\pi \, \varepsilon_a^{1/2} \, k^2 \, r^2} \times$$

$$\times \{\cos^2\varphi \, \tau_{n1}^2(\theta) + \sin^2\varphi \, \pi_{n1}^2(\theta)\}. \quad (11)$$

In the case of multimode excitation of the SRS, the Eqs. (9) and (10) take the form

$$\mathbf{E}_\theta(\mathbf{r}, t) = \frac{(\varepsilon_a - 1)}{2k_a r} \exp\{i\omega_S t - ikr\} \cos\varphi \times$$

$$\times \sum_n (i)^n (2n+1) A_{Mn}(t, k_a a) \, \tau_{n1}(\theta) \, \Re_{1(nn)}; \quad (12)$$

$$\mathbf{E}_\varphi(\mathbf{r}, t) = -\frac{(\varepsilon_a - 1)}{2k_a r}\exp\{i\omega_S t - ikr\}\sin\varphi \times$$

$$\times \sum_n (i)^n (2n+1) A_{Mn}(t, k_a a)\, \pi_{n1}(\theta)\Re_{1(nn)}. \quad (13)$$

Equation (11) also includes the sum over all interacting modes. The contribution from every mode to the total intensity of scattering is proportional to the volume occupied by the mode and to the Q-factor of a partial resonance, what is taken into account in the coefficient A_{Mn} :

$$I(\theta, \varphi, t) = \sum_n (I_{\theta n} + I_{\varphi n}) = \frac{c(\varepsilon_a - 1)^2}{32\pi^2 \varepsilon_a^{1/2} k^2 r^2} \times$$

$$\times \sum_n \sum_m (2n+1)(2m+1) A_{Mn} A^*_{Mn} \times$$

$$\times \{\cos^2\varphi\, \tau_{n1}\tau^*_{m1}{}^2 + \sin^2\varphi\, \pi_{n1}\pi^*_{m1}\}\Re_{1(nn)}\, \Re^*_{1(mm)}. \quad (14)$$

As seen from Eq. (14), the equation for the total intensity involves the terms of the form $(\tau_{n1}\tau^*_{m1})$ $(\Re_{1(nn)}\, \Re_{1(mm)})$ besides the non-coherent contributions of individual resonance modes. These terms take account of the coherent interaction of individual partial harmonics. The degree of this interaction depends on the spatial overlapping of the modes (the coefficients $\Re_{1(nn)}$). As calculations show, this degree is maximum if the resonance modes have the same order. At the same time, it is just these "cross" terms that introduce asymmetry into the angular distribution of the scattered radiation intensity.

Results of numerical calculations

The main difficulty in performing model calculations of the angular distribution of intensity of the stimulated scattering in the case of multimode excitation is caused by the participation of modes with different values of the mode index n and the order M in this process. Consequently, all these modes have different Q-factors and occupy different mode volumes. The problem of competition of modes in the process of multimode excitation of stimulated scattering or, in other words, the question on which mode dominates over others is still practically not studied. That is why there is no a unique criterion allowing even relative determination of the amplitude A_{Mn}. In this connection it is worth, in our opinion, assuming that all modes interacting in the particle have equal amplitudes, that is, the equality

$$(2n_1 + 1)\left|A_{Mn1}(t, k_a a)\, \Re_{1(n_1 n_1)}\right| =$$
$$= (2n_2 + 1)\left|A_{Mn2}(t, k_a a)\Re_{2(n_2 n_2)}\right| = \ldots . \quad (15)$$

is valid.

For numerical estimates of the intensity of a scattered wave by Eq. (14), different combinations of the resonance modes having frequencies close to $\omega_S = 15400\ \text{cm}^{-1}$ (Table 1) have been determined. The frequency ω_S corresponds to the center of Stokes line in the Raman spectrum of water irradiated with the radiation at $\lambda = 0.532$ μm.

Table 1

Resonance mode	Resonance radius a_0, μm	Radiation Q-factor of the mode	Halfwidth of the resonance curve c_{nl}	$\frac{1}{a_0}\lvert\Re_{1(nn)}\rvert$, $\frac{1}{a_0}\lvert\Re_{2(nn)}\rvert$
$\boldsymbol{TE^3_{70}}$	**6.842019**	**429.79**	$\mathbf{1.53\cdot10^{-1}}$	**0.306**
TE^5_{62}	6.873510	45.81	1.45	0.310
TE^4_{66}	6.866961	84.99	$7.81\cdot10^{-1}$	0.310
TE^2_{75}	6.857325	$1.95\cdot10^4$	$3.38\cdot10^{-3}$	0.308
TE^1_{81}	6.855499	$1.89\cdot10^7$	$3.48\cdot10^{-6}$	0.308
$\boldsymbol{TM^3_{70}}$	**6.868196**	**286.11**	$\mathbf{2.32\cdot10^{-1}}$	$\mathbf{0.841\cdot10^{-1}}$
TM^5_{62}	6.880742	17.41	3.82	$0.753\cdot10^{-1}$
TM^4_{66}	6.879255	46.89	1.41	$0.753\cdot10^{-1}$
TM^2_{74}	6.814307	$1.13\cdot10^4$	$5.81\cdot10^{-3}$	$0.669\cdot10^{-1}$
TM^2_{75}	6.897084	$1.35\cdot10^4$	$4.93\cdot10^{-3}$	$0.743\cdot10^{-1}$
TM^1_{80}	6.821987	$1.09\cdot10^7$	$6.03\cdot10^{-6}$	$0.744\cdot10^{-1}$
$\boldsymbol{TE^3_{70}}$	**6.842019**	**429.79**	$\mathbf{1.53\cdot10^{-1}}$	**0.306**
TM^5_{62}	6.880742	17.41	3.82	$0.753\cdot10^{-1}$
TM^4_{66}	6.879255	46.89	1.41	$0.753\cdot10^{-1}$
TM^2_{74}	6.814307	$1.13\cdot10^4$	$5.81\cdot10^{-3}$	$0.669\cdot10^{-1}$
TM^2_{75}	6.897084	$1.35\cdot10^4$	$4.93\cdot10^{-3}$	$0.743\cdot10^{-1}$
TM^1_{80}	6.821987	$1.09\cdot10^7$	$6.03\cdot10^{-6}$	$0.744\cdot10^{-1}$
$\boldsymbol{TM^3_{70}}$	**6.868196**	**286.11**	$\mathbf{2.32\cdot10^{-1}}$	$\mathbf{0.841\cdot10^{-1}}$
TE^5_{62}	6.873510	45.81	1.45	0.310
TE^4_{66}	6.866961	84.99	$7.81\cdot10^{-1}$	0.310
TE^2_{75}	6.857325	$1.95\cdot10^4$	$3.38\cdot10^{-3}$	0.308
TE^1_{81}	6.855499	$1.89\cdot10^7$	$3.48\cdot10^{-6}$	0.308

Figure 3 demonstrates the theoretically calculated results on the angular dependence of SRS at unimodal and multimode excitation in a water droplet with the radius $a_0 = 6.86$ μm (all curves are smoothed to be more descriptive). As seen from Fig. 3, the directional pattern is practically symmetric in the case of SRS supported by only one resonance mode (the TM^3_{70} mode in this case). This can be explained by the corresponding symmetry of the internal emitting field in the droplet (Fig. 4).

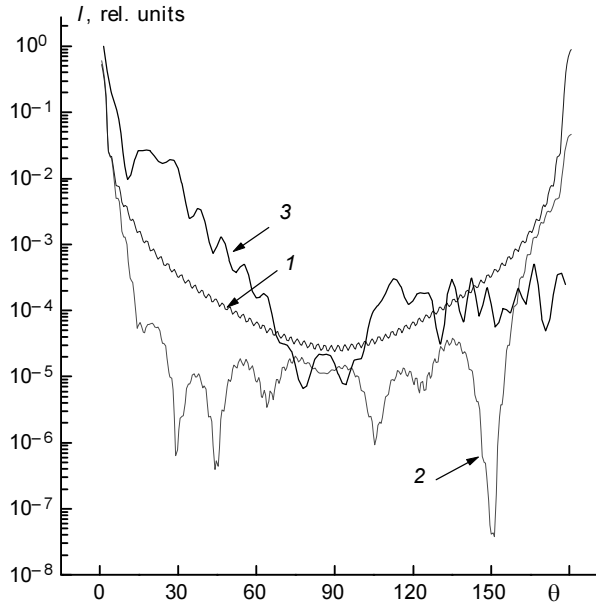

Fig. 3. Angular distribution of the intensity of SRS from a water droplet in the cases of excitation of the TE^3_{70} resonance mode (*1*) and the combination of the TE^3_{70}, TE^5_{62}, TE^4_{66}, TE^2_{75}, and TE^1_{81} modes (*2*). Curve *3* is for the elastic scattering.

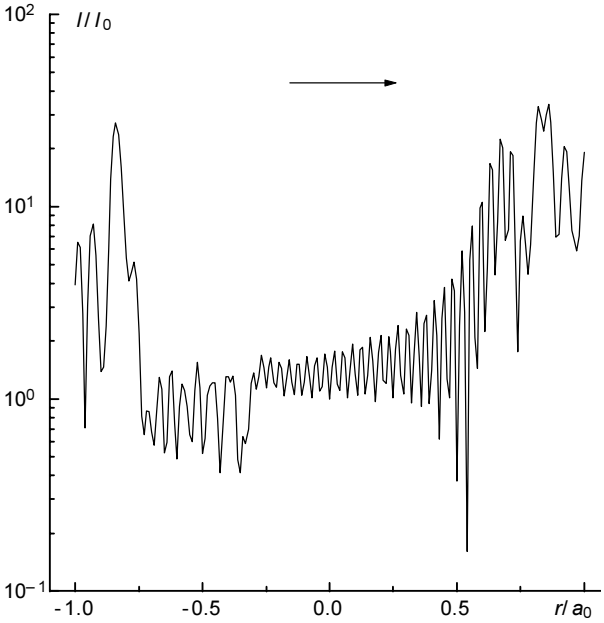

Fig. 4. Distribution of the intensity of the internal optical field in a droplet for the TE^3_{70} resonance mode. The horizontal arrow shows the incidence direction of the pump radiation.

At the same time, the angular distribution of Raman radiation has the maximum in the forward and backward directions about the direction of incident radiation and the minimum along the orthogonal direction; it is symmetric with the period multiple of $\pi/2$. In contrast to the directional pattern of the elastic scattering (curve *3* in Fig. 3), the directional pattern of SRS is more uniform because of the absence of the Raman field component due to diffraction on the particle.

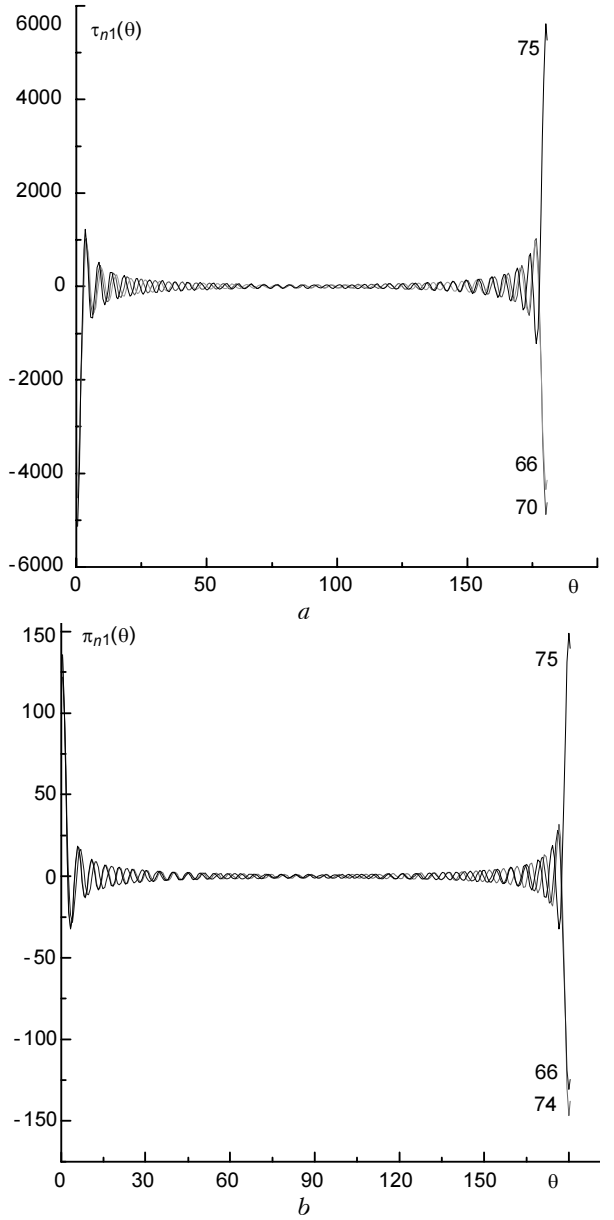

Fig. 5. Behavior of the angular functions for the *TE*-modes (*a*) and *TM*-modes (*b*). The figures at the curves show the mode index *n*.

At multimode excitation of the SRS, which involves coherent combining of several resonance modes, the directional pattern becomes significantly asymmetric. Besides, it turns out that the degree of its

uniformity significantly depends on which modes support the scattering process. As seen from Fig. 5, the behavior of the angular functions $\pi_{n1}(\theta)$ and $\tau_{n1}(\theta)$, that determine the directional pattern of the scattered waves outside the particle, differs for the modes with even and odd values of the mode index n. Thus, under certain conditions, combining of modes with even numbers results in a significant increase in the amplitude of the resulting wave in the backward direction. At the same time, combining of modes with even and odd values of n leads to a decrease in the backscattering signal.

We have considered different combinations of excitation of the resonance modes in a water droplet. For example, in the case of excitation of *TE*-modes in a droplet, the frequencies of the TE_{62}^5, TE_{66}^4, TE_{75}^2, and TE_{81}^1 modes are close to the frequency of the main resonance TE_{70}^3 mode (see Table 1). The SRS directional pattern for this combination is asymmetric being elongated in the forward direction (see Fig. 3). For the sake of comparison, Fig. 6 shows the angular distribution of the scattered radiation for the combination of the TE_{70}^5, TE_{74}^4, TE_{78}^3, TE_{83}^2, TE_{84}^2, and TE_{90}^1 resonance modes. As seen from Fig. 6, the SRS directional pattern in this case is more symmetric, because modes of mostly even orders participate in the process. The values of the signal intensity along the directions at 0 and 180° differ only by 1.5 times. Quite similar dependence $I(\theta)$ is observed for the case of interaction among the *TM*-modes in the droplet.

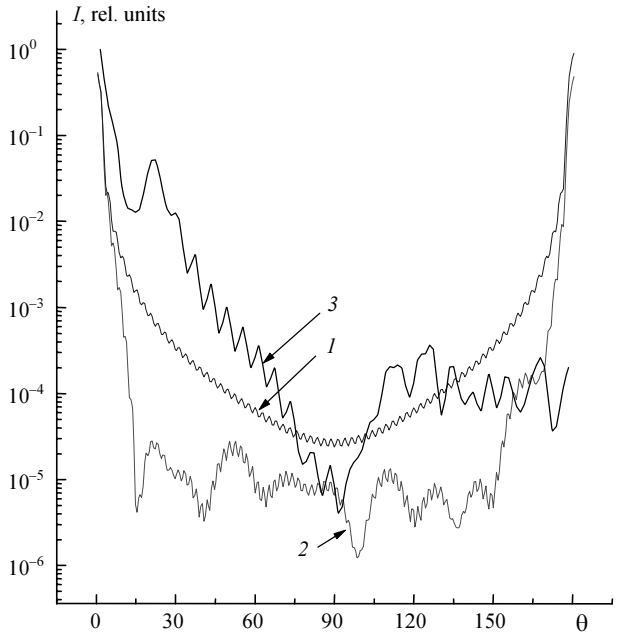

Fig. 6. Angular distribution of the intensity of SRS from a water droplet in the case of excitation of TE_{70}^5 resonance mode (*1*) and the combination of the TE_{70}^5, TE_{74}^4, TE_{78}^3, TE_{83}^2, TE_{84}^2, and TE_{90}^1 modes (*2*). Curve *3* shows the directional pattern of the elastic scattering.

Besides, we have calculated the distribution of the field far from the particle in the case of excitation of the combination of both the *TE*- and *TM*-modes in the droplet. Figure 7 shows the corresponding directional patterns for the case of interaction among the TM_{70}^3, TE_{65}^5, TE_{66}^4, TE_{75}^2, and TE_{81}^1 resonance modes in a water droplet. As mentioned above, the formation of the SRS directional pattern is governed by the behavior of the angular functions and by the parity of the mode index n. For this combination of modes the directional pattern is asymmetric and, in contrast to the case of interaction of modes having the same polarization, close to the intensity distribution for the case with a single resonance mode.

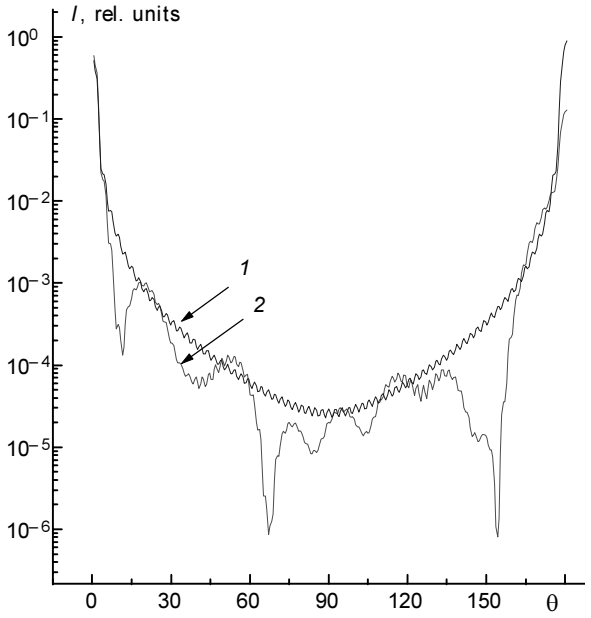

Fig. 7. Angular distribution of the SRS intensity at the unimodal (TE_{70}^3 resonance mode) excitation (*1*) and multimode (combination of the *TE*- and *TM*-modes) excitation (*2*).

It is also worth noting the fact that the angular behavior of the scattered wave intensity at multimode excitation is significantly sharper being primarily localized near the angles $\theta = 0$ and 180°. In other directions, mutual suppression of the resonance modes with different values of the mode index takes place. This result follows from the accepted approximation on equal amplitudes of the interacting resonance modes.

The above results of theoretical studies are, in general, in a good agreement with the experimental data on the angular structure of the field of SRS induced by a laser radiation in isolated ethanol droplets.[18]

Conclusion

In this paper we have considered some peculiarities in the angular distribution of the field of stimulated scattering from transparent spherical micrometer-sized particles exposed to high-power laser radiation. The equations for the intensity of scattered waves at unimodal and multimode excitation of the SRS were derived. It was found that

the unimodal excitation always results in a symmetric angular distribution of the SRS intensity in the forward and backward directions. At the same time, participation of modes with close frequencies in the process of development of the SRS wave may result (at certain combinations of the modes) in asymmetry of the SRS directional pattern. The directional pattern in such a case is elongated in the forward direction, and the forward–to-bacward intensity ratio is about 10 to 20. Such a dependence, at the multimode excitation, is caused by the coherent interaction between the fields of natural modes of a particle resulting in their mutual amplification in some directions and mutual suppression in others.

References

1. O.A. Bukin, U.Kh. Kopvillem, S.Yu. Stolyarchuk, and V.A. Tyapkin, Zh. Prikl. Spektrosk. **38**, 778–785 (1983).
2. U.Kh. Kopvillem, O.A. Bukin, V.M. Chudinovskii, et al., Opt. Spektrosk. **59**, No. 2, 306–310 (1985).
3. G. Schweiger, Part. Charact. **4**, 67–73 (1987).
4. W.P. Acker et al., Appl. Phys. **B51**, 9–16 (1990).
5. P.R. Conwell, C.K. Rushforth, R.E. Benner, and S.C. Hill, J. Opt. Soc. Am. A **1**, No. 12, 1181–1187 (1984).
6. Y. Yamamoto and R. Slusher, Phys. Today, No. 6, 66–73 (1993).
7. A.N. Oraevskii, M. Skalni, and V.L. Velichanskii, Kvant. Elektron. **25**, No. 3, 211–216 (1998).
8. B. Little, H. Haus, E. Ippen, G. Steinmeyer, and E. Thoen, Optics and Photonics News **9**, No. 12, 32–33 (1998).
9. T. Baer, Opt. Lett. **12**, No. 6, 392–394 (1987).
10. Yu.E. Geints and A.A. Zemlyanov, Atmos. Oceanic Opt. **9**, No. 7, 575–577 (1996).
11. J.B. Snow, S.-H. Quan, and R.K. Chang, Opt. Lett. **10**, No. 1, 37–39 (1985).
12. J.A. Stretton, *Theory of Electromagnetism* (OGIZ, Moscow–Leningrad, 1948), 540 pp.
13. K.S. Shifrin, *Scattering of Light in a Turbid Medium* (Gos. Izdat. Tekhniko-Teor. Lit., Moscow–Leningrad, 1951), 288 pp.
14. H. Chew, P.J. McNulty, and M. Kerker, Phys. Rev. A **13**, No. 1, 396–404 (1976).
15. B.R. Johnson, J. Opt. Soc. Am. **10**, No. 2, 343–350 (1993).
16. Yu.E. Geints, A.A. Zemlyanov, and E.K. Chistyakova, Atmos. Oceanic Opt. **11**, No. 1, 30–38 (1998).
17. M. Abramovits and I. Stigan, eds., *Reference Book on Special Functions with Formulas, Plots, and Mathematical Tables* (Nauka, Moscow, 1979), 830 pp.
18. R.G. Pinnick, A. Biswas, R.L. Armstrong, et al., Opt. Lett. **13**, No. 12, 1099–1101 (1988).